Perceptual difficulty modulates the direction of information flow in familiar face recognition

Hamid Karimi-Rouzbahani[1*], Farzad Remezani[2], Alexandra Woolgar[1,3], Anina Rich[1], Masoud Ghodrati[4*]

[1]Perception in Action Research Centre and Department of Cognitive Science Macquarie University, Australia

[2]Department of Computer Science, School of Mathematics, Statistics, and Computer Science, University of Tehran, Iran

[3]Medical Research Council Cognition and Brain Sciences Unit, University of Cambridge, UK

[4]Neuroscience Program, Biomedicine Discovery Institute, Monash University, Australia

* to whom correspondence should be addressed.

Abstract

Humans are fast and accurate when they recognize familiar faces. Previous neurophysiological studies have shown enhanced representations for the dichotomy of familiar vs. unfamiliar faces. As familiarity is a spectrum, however, any neural correlate should reflect graded representations for more vs. less familiar faces along the spectrum. By systematically varying familiarity across stimuli, we show a neural familiarity spectrum using electroencephalography. We then evaluated the spatiotemporal dynamics of familiar face recognition across the brain. Specifically, we developed a novel informational connectivity method to test whether peri-frontal brain areas contribute to familiar face recognition. Results showed that feed-forward flow dominates for the most familiar faces and top-down flow was only dominant when sensory evidence was insufficient to support face recognition. These results demonstrate that perceptual difficulty and the level of familiarity influence the neural representation of familiar faces and the degree to which peri-frontal neural networks contribute to familiar face recognition.

***Keywords*:** Face Recognition, Familiar Faces, Multivariate Pattern Analysis (MVPA), Representational Similarity Analysis (RSA), Informational Brain Connectivity

Introduction

Faces are crucial for our social interactions, allowing us to extract information about identity, gender, age, familiarity, intent and emotion. Humans categorize familiar faces more quickly and accurately than unfamiliar ones, and this advantage is more pronounced under difficult viewing conditions, where categorizing unfamiliar faces often fails (Ramon and Gobbini, 2018; Young and Burton, 2018). The neural correlates of this behavioral advantage suggest an enhanced representation of familiar over unfamiliar faces in the brain (Dobs et al., 2019; Landi and Freiwald, 2017). Here, we focus on addressing two major questions about familiar face recognition. First, whether there is a "familiarity spectrum" for faces in the brain with enhanced representations for more vs. less familiar faces along the spectrum. Second, whether higher-order frontal brain areas contribute to familiar face recognition, as they do to object recognition (Bar et al,. 2006; Summerfield et al., 2006; Goddard et al., 2016; Karimi-Rouzbahani et al., 2019), and whether levels of face familiarity and perceptual difficulty (as has been suggested previously (Woolgar et al., 2011; Woolgar et al., 2015)) impact the involvement of peri-frontal cognitive areas in familiar face recognition.

One of the main limitations of previous studies, which hinders our progress in answering our first question, is that they mostly used celebrity faces as the familiar category (Ambrus et al., 2019; Collins et al., 2018; Dobs et al., 2019). As familiar faces can range widely from celebrity faces to highly familiar ones such as family members, relatives, friends, and even one's own face (Ramon and Gobbini, 2018), these results might not reflect the full familiarity spectrum. A better understanding of familiar face recognition requires characterizing the computational steps and representations for sub-categories of familiar faces, including personally familiar, visually familiar, famous, and experimentally learned faces. Such face categories might not only differ in terms of their visual representations and their information coding, but also the availability of personal knowledge, relationships, and emotions associated with the identities in question (Ramon and Gobbini, 2018). These categories may, therefore, vary in terms of the potential for top-down influences in the process. Importantly, while a few functional magnetic resonance imaging (fMRI) studies have investigated the differences between different

levels of familiar faces (Gobbini et al., 2004; Landi and Freiwald, 2017; Leibenluft et al., 2004; Ramon et al., 2015; Sugiura et al., 2015; Taylor et al., 2009), there are no studies that systematically compare the temporal dynamics of *information processing* across this familiarity spectrum. Specifically, while event-related potential (ERP) analyses have shown amplitude modulation by levels of face familiarity (Henson et al., 2008; Kaufmann et al., 2009; Schweinberger et al., 2002; Huang et al., 2017), they remain silent about whether more familiar faces are represented better or worse than less familiar faces - amplitude modulation does not necessarily mean that information is being represented. To address this issue, we can use multivariate pattern analysis (MVPA or decoding; Ambrus et al., 2019; Karimi-Rouzbahani et al., 2017a) to compare the amount of *information* in each of the familiarity levels.

In line with our second question, recent human studies have compared the neural dynamics for familiar versus unfamiliar face processing using the high temporal resolution of electroencephalography (EEG; Ambrus et al., 2019; Collins et al., 2018) and magnetoencephalography (MEG; Dobs et al., 2019). These studies have found that familiarity affects the initial time windows of face processing in the brain, which are generally attributed to the feed-forward mechanisms of the brain. In particular, they have explored the possibility that the face familiarity effect occurs because these faces have been seen repeatedly, leading to the development of low-level representations for familiar faces in the occipito-temporal visual system. This in turn facilitates the flow of familiar face information in a bottom-up feed-forward manner from the occipito-temporal to the frontal areas for recognition (di Oleggio Castello and Gobbini, 2015; Ramon et al., 2015; Ellis et al., 1979; Young and Burton, 2018). On the other hand, studies have also shown the role of frontal brain areas in facilitating the processing of visual inputs (Bar et al., 2006; Kveraga et al., 2007; Goddard et al., 2016; Karimi-Rouzbahani et al., 2019), such as faces (Kramer et al., 2018; Summerfield et al., 2006), by feeding back signals to the face-selective areas in the occipito-temporal visual areas, particularly when the visual input is ambiguous (Summerfield et al., 2006) or during face imagery (Mechelli et al., 2004; Johnson et al., 2007). These top-down mechanisms, which were localized in medial frontal cortex, have been suggested (but not quantitatively supported) to reflect feedback of (pre-existing) face templates, against which the input faces are compared for correct

recognition (Summerfield et al., 2006). Despite the large literature of face recognition, the roles of the feed-forward (i.e. peri-occipital to peri-frontal) and feedback (i.e. peri-frontal to peri-occipital) brain mechanisms, and their possible temporal interactions, in familiar face recognition have remained ambiguous. We develop novel connectivity methods to track the flow of information along the feed-forward and feedback mechanisms and assess the role of these mechanisms in familiar face recognition.

One critical aspect of the studies that successfully detected top-down peri-frontal to peri-occipital feedback signals (Bar et al., 2006; Summerfield et al., 2006; Goddard et al., 2016) has been the *active* involvement of the participant in a task. In recent E/MEG studies reporting support for a feed-forward explanation of the face familiarity effect, participants were asked to detect target faces (Ambrus et al., 2019) or find a match between faces in series of consecutively presented faces (Dobs et al., 2019). This makes familiarity irrelevant to the task of the participant. Such indirect tasks may reduce the involvement of top-down familiarity-related feedback mechanisms, as was demonstrated by a recent study (Kay et al., 2017), which found reduced feedback signals (from intraparietal to ventro-temporal cortex) when comparing fixation versus an active task in an fMRI study. Therefore, to answer our first research question and fully test the contribution of feedback to the familiarity effect, we need active tasks that are affected by familiarity.

Timing information is also crucial in evaluating the flows of feed-forward and feedback information as these processes often differ in the temporal dynamics. With the advent of the concept of informational connectivity analysis, we now have the potential to examine the interaction of information between feed-forward and feedback mechanisms to characterize their potential spatiotemporal contribution to familiar face recognition (Goddard et al., 2016; Goddard et al., 2019; Anzellotti and Coutanche, 2018; Basti et al., 2020; Karimi-Rouzbahani et al., 2020). However, this requires novel methods to track the flow of familiarity information from a given brain area to a destination area and link this flow to the behavioural task goals to confirm its biological relevance. Such analyses can provide valuable insights for understanding the neural mechanisms underlying familiar face recognition in humans.

In our study, participants performed a familiar vs. unfamiliar face categorization task on sequences of images selected from four face categories (i.e., unfamiliar, famous, self, and personally familiar faces), with dynamically updating noise patterns, while their EEG data were recorded. By varying the signal-to-noise ratio of each image sequence using perceptual coherence, we were able to investigate how information for the different familiar categories gradually builds up in the electrical activity recordable by scalp electrodes, and how this relates to the amount of sensory evidence available in the stimulus (perceptual difficulty). The manipulation of sensory evidence also allowed us to investigate when, and how, feedback information flow affects familiar face recognition. Using univariate and multivariate pattern analyses, representational similarity analysis (RSA) and a novel informational connectivity analysis method, we reveal the temporal dynamics of neural representations for different levels of face familiarity.

Our results show that self and personally familiar faces lead to higher perceptual categorization accuracy and enhanced representation in the brain even when sensory information is limited while famous (visually familiar) and unfamiliar face categorization is only possible in high-coherence conditions. Importantly, our extension of information flow analysis reveals that in high-coherence conditions the feed-forward sweep of face category information processing is dominant, while at lower coherence levels the exchange of face category information is dominated by feedback. The change in dominance of feedback versus feed-forward effects as a function of coherence level supports a dynamic exchange of information between higher-order (frontal) cognitive and visual areas depending on the amount of sensory evidence.

Results

We designed a paradigm to study how the stimulus- and decision-related activations for different levels of face familiarity build up during stimulus presentation and how these built-up activations relate to the amount of sensory evidence about each category. We recorded EEG data from human participants (n=18) while they categorized

face images as familiar or unfamiliar. We varied the amount of sensory evidence by manipulating the phase coherence of images on different trials (Figure 1A). In each 1.2 s (max) sequence of image presentation (trial), the pattern of noise changed in each frame (16.7 ms) while the face image and the overall coherence level remained the same. Familiar face images (120) were selected equally from celebrity faces, photos of the participants' own face, and personally familiar faces (e.g., friends, family members, relatives of the participant) while unfamiliar face images (120) were completely unknown to participants before the experiment. Within each block of trials, familiar and unfamiliar face images with different coherence levels were presented in random order.

Levels of face familiarity are reflected in behavioral performance

We quantified our behavioral results using accuracy and reaction times on correct trials. Specifically, accuracy was the percentage of images correctly categorized as either familiar or unfamiliar. All participants performed with high accuracy (>92%) at the highest phase coherence (55%), and their accuracy was much lower (~62%) at the lowest coherence (22%; $F(3,272)=75.839$, $p<0.001$; Figure 1B). The correct reaction times show that participants were faster to categorize the face at high phase coherence levels than lower ones ($F(3,272)=65.797$, $p<0.001$, main effect; Figure 1C). We also calculated the accuracy and reaction times for the sub-categories of the familiar category separately (i.e. famous, personally familiar and self). Note that the task was two-alternative forced-choice between familiar vs. unfamiliar faces, so participants were not specifically asked to categorize the sub-categories. The calculated accuracy here is the percentage of correct responses within each of these familiar sub-categories. The results show a gradual increase in accuracy as a function of phase coherence and familiarity (Figure 1D, two-way ANOVA. factors: coherence level and face category. Face category main effect: $F(2,408)=188.708$, $p<0.001$, coherence main effect: $F(3,408)= 115.977$, $p<0.001$, and interaction: $F(6,408)=12.979$, $p<0.001$), with the highest accuracy in categorizing their own (self), then personally familiar, and finally famous (or visually familiar) faces. The reaction time analysis also showed a similar pattern where participants were fastest to

177 categorize self faces, then personally familiar and famous faces (Figure 1E, two-way
178 ANOVA, factors: coherence level and face category. Face category main effect:
179 $F(2,404)=174.063$, $p<0.001$, coherence main effect: $F(3,404)= 104.861$, $p<0.001$, and
180 interaction: $F(6,404)=17.051$, $p<0.001$). All reported p-values were corrected for multiple
181 comparisons using Bonferroni correction.

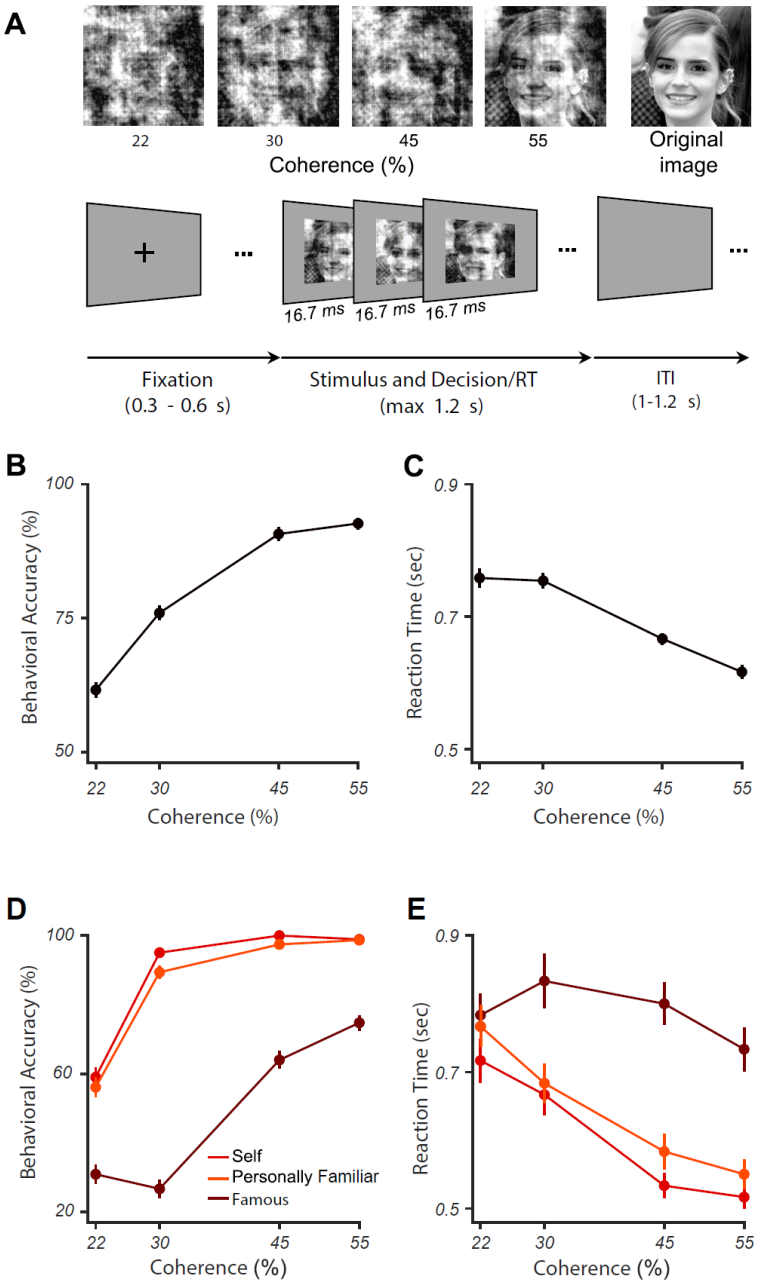

182

183 **Figure 1. Experimental design and behavioral results for familiar vs. unfamiliar face categorization.**
184 (A) Upper row shows a sample face image (from the famous category) at the four different phase coherence

levels (22, 30, 45, and 55%) used in this experiment, in addition to the original image (not used). Lower row shows schematic representation of the experimental paradigm. In each trial, a black fixation cross was presented for 300-600 ms (randomly selected). Then, a noisy and rapidly updating (every 16.7 ms) stimulus of a face image (unfamiliar, famous, personally familiar, or self), at one of the four possible phase coherence levels, was presented until response, for a maximum of 1.2 s. Participants had to categorize the stimulus as familiar or unfamiliar by pressing one of two buttons (button mappings swapped across the two sessions, counterbalanced across participants). There was then a variable intertrial interval (ITI) lasting between 1-1.2 s (chosen from a uniform random distribution; see a demo of the task here *https://osf.io/n7b8f/*). (B) Mean behavioral accuracy for face categorization across all stimuli, as a function of coherence levels; (C) Median reaction times for correctly categorized face trials across all conditions, as a function of coherence levels. (D) and (E) show the results for different familiar face sub-categories. Error bars in all panels are the standard error of the mean across participants.

Is there a "familiarity spectrum" for faces in the brian?

Our behavioral results showed that there is a graded increase in participants' performance as a function of familiarity level - i.e., participants achieve higher performance if the faces are more familiar to them. In this section we address the first question of this study about whether we can find a familiarity spectrum in neural activations, using both the traditional univariate and novel multi-variate analyses of EEG.

Event-related potentials reflect behavioral familiarity effects

As an initial, more traditional, pass at the data, we explored how the neural responses were modulated by different levels of familiarity and coherence by averaging event-related potentials (ERP) across participants for different familiarity levels and phase coherences (Figure 2B). This is important as recent work failed to capture familiar face identity information from single electrodes (Ambrus et al., 2019). At high coherence, the averaged ERPs, obtained from a representative centroparietal electrode (CP2), where previous studies have found differential activity for different familiarity levels (Henson et al., 2008; Kaufmann et al., 2009; Huang et al., 2017), demonstrated an early, evoked response, followed by an increase in the amplitude proportional to familiarity levels. This showed that self faces elicited the highest ERP amplitude, followed by personally familiar, famous, and unfamiliar faces (Figure 2B for 55% phase coherence). This observation of late differentiation between familiarity levels at later time points seems to support

217 evidence accumulation over time, which is more pronounced at higher coherence levels
218 where the brain had access to reliable information.

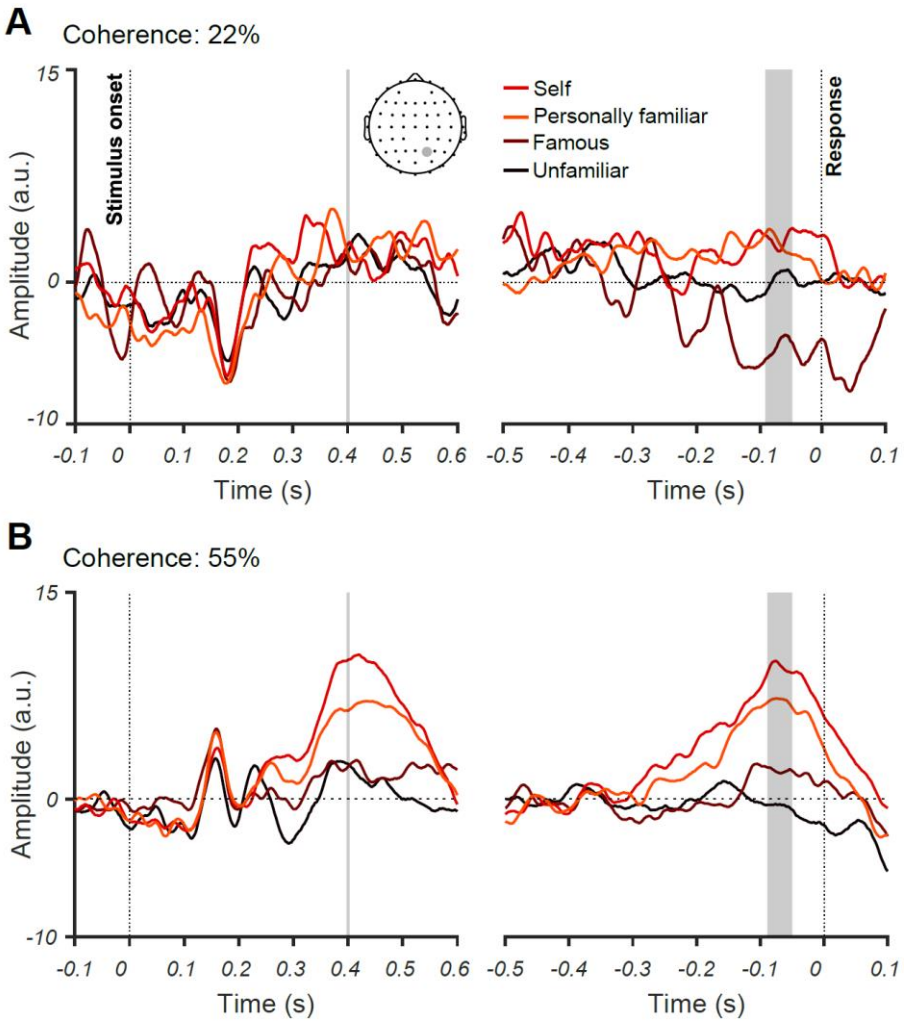

219

220 **Figure 2. The effect of familiarity and sensory evidence on event-related potentials (ERPs).** Averaged
221 ERPs for 22% (A) and 55% (B) phase coherence levels and four face categories across all participants for
222 an electrode at a centroparietal site (CP2). Note that the left panels show stimulus-aligned ERPs while the
223 right panel shows response-aligned ERPs. Shaded areas show the time windows, when the absolute ERP
224 differences between the four face categories were significantly ($p<0.05$) higher in the 55% vs. 22%
225 coherence levels. The significance was evaluated using one-sided unpaired *t*-test with correction for
226 multiple comparisons across time. The differences were significant at later stages of stimulus processing
227 around 400 ms post-stimulus onset and <100 ms before the response was given by the participant in the
228 stimulus- and response-aligned analyses, respectively.

229

230 We also observed a similar pattern between the ERPs of different familiarity levels
231 at the time of decision (just before the response was made). Such systematic

differentiation across familiarity levels was lacking at the lowest coherence level, where the amount of sensory evidence, and behavioral performance, were low (c.f. Figure 2A for 22% phase coherence; shaded areas, evaluated using unpaired one-sided *t*-test $p<0.05$, Bonferroni-corrected for multiple comparisons across time). These results reveal the neural correlates of perceptual differences in categorizing different familiar face categories under perceptually difficult conditions.

Dynamics of neural representation and evidence accumulation for different face familiarity levels

Our results so far are consistent with previous event-related studies showing that the amplitude of ERPs is modulated by the familiarity of the face (Henson et al., 2008; Kaufmann et al., 2009; Schweinberger et al., 2002; Huang et al., 2017). However, more modulation of ERP amplitude does not necessarily mean more information. To address this issue, we used multivariate pattern and representational similarity analyses on these EEG data to quantify the time course of familiar vs. unfamiliar face processing. Compared to traditional single-channel (univariate) ERP analysis, MVPA allows us to capture the whole-brain widespread and potentially subtle differences between the activation dynamics of different familiarity levels (Ambrus et al., 2019; Dobs et al., 2019). Specifically, we asked: (1) how the coding dynamics of stimulus- and response-related activities change depending on the level of face familiarity; and (2) how manipulation of sensory evidence (phase coherence) affects neural representation and coding of different familiarity levels.

To obtain the temporal evolution of familiarity information across time, at each time point we trained the classifier to discriminate between familiar and unfamiliar faces. Note that the mapping between response and fingers were swapped from the first session to the next (counterbalanced across participants) and the data were collapsed across the two sessions for these analyses, which ensures the motor response cannot drive the classifier. We trained the classifier using 90% of the trials and tested them on the left-out 10% of data using a standard 10-fold cross-validation procedure (see *Methods*). This

analysis used only correct trials. Our decoding analysis showed that, up until ~200 ms after stimulus onset, decoding accuracy is near chance for all coherence levels (Figure 3A). The decoding accuracy then gradually increases over time and peaks around 500 ms post-stimulus for the highest coherence level (55%) but remains around chance for the lower coherence level (22%, Figure 3A). The accuracy for intermediate coherence levels (30% and 45%) falls between these two bounds but only reaches significance above chance for the 45% coherence level. This ramping up temporal profile suggests an accumulation of sensory evidence in the brain across the time course of stimulus presentation, which has a processing time that depends on the strength of the sensory evidence (Hanks and Summerfield, 2017; Philiastides et al., 2006).

To examine if neural responses can be decoded at finer categorization levels, we separately calculated the decoding accuracy for each of the familiar face sub-categories (after collapsing the data across all coherence levels and decoding familiar vs. unfamiliar trials as explained above): unfamiliar, famous, self and personally familiar faces (Figure 3B). The decoding accuracy was highest for self faces, both for stimulus- and response-aligned analyses, followed by personally familiar, famous and unfamiliar faces. Accuracy for the response-aligned analysis shows that the decoding gradually increased to peak decoding ~100 ms before the response was given by participants. This temporal evolution of decoding accuracy begins after early visual perception and rises in proportion to the amount of the face familiarity.

Low-level stimulus differences between conditions could potentially drive the differences between categories observed in both ERP and decoding analyses (e.g., familiar faces being more frontal than unfamiliar faces, leading to images with brighter centers and, therefore, separability of familiar from unfamiliar faces using central luminance of images; Dobs et al., 2019; Ambrus et al., 2019). To address such potential differences, we carried out a supplementary analysis using RSA (Supplementary Materials), which showed that any such differences between images could not drive the differentiation between categories.

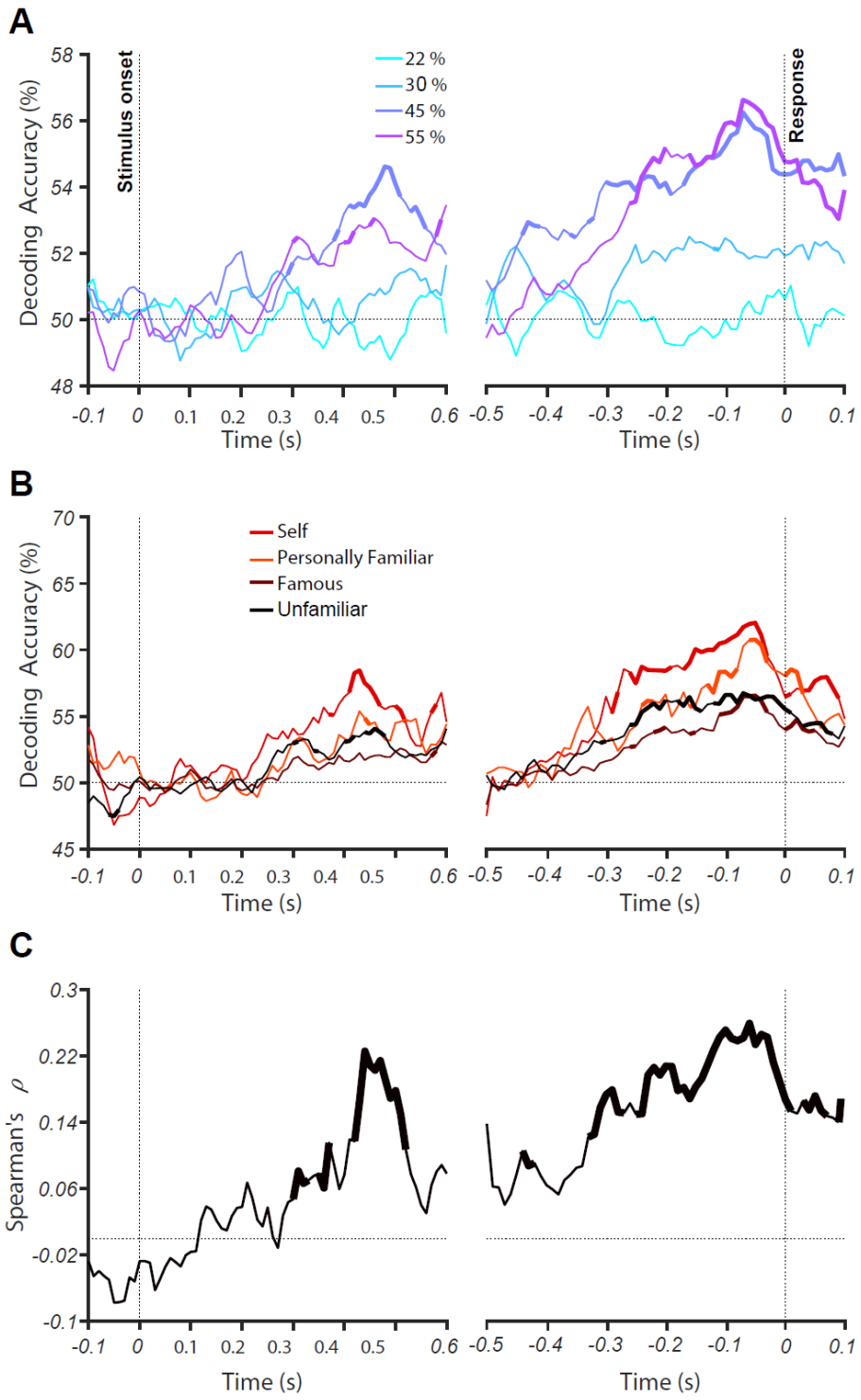

Figure 3. Decoding of face familiarity from EEG signals. (A) Time course of decoding accuracy for familiar versus unfamiliar faces from EEG signals for four different phase coherence levels (22%, 30%, 45%, and 55%). (B) Time course of decoding accuracy for four face categories (i.e., unfamiliar, famous, self and personally familiar faces) from EEG signals collapsed over phase coherence levels. The chance accuracy is 50%. Thickened lines indicate the time points when the accuracy was significantly above chance level (sign rank test, FDR corrected across time, $p<0.05$). (C) Correlation between behavioral

297 performance and decoding accuracy (across all conditions) over time. Thickened lines indicate the time
298 points when the correlation was significant. The left panels show the results for stimulus-aligned analysis
299 while the right panels show the results for response-aligned analysis (averaged over 18 participants).

300

301 To determine whether the dynamics of decoding during stimulus presentation are
302 associated with the perceptual task, as captured by our participants' behavioral
303 performance, we calculated the correlation between decoding accuracy and perceptual
304 performance. For this, we calculated the correlation between 16 data points from
305 decoding accuracy (4 face categories * 4 phase coherence levels) and their
306 corresponding behavioral accuracy rates, collapsed over participants. The correlation
307 peaked ~500 ms post-stimulus (Figure 3C), which was just before the response was
308 given. This is consistent with an evidence accumulation mechanism determining whether
309 to press the button for 'familiar' or 'unfamiliar', which took another ~100 ms to turn into
310 action (finger movement).

311

312 Do higher-order peri-frontal brain areas contribute to familiar face
313 recognition?

314 In this section we address the second question of this study about whether peri-
315 frontal brain areas contribute to the recognition of familiar faces in the human brain using
316 a novel model-based connectivity analyses on EEG.

317

318 Task difficulty and familiarity level affect information flow across the brain

319 We investigated how the dynamics of feed-forward and feedback information flow
320 changes during the accumulation of sensory evidence and the evolution over a trial of
321 neural representations of face images. We developed a novel connectivity method based
322 on RSA to quantify the relationships between the evolution of information based on peri-
323 occipital EEG electrodes and those of the peri-frontal electrodes. As an advantage to

previous Granger causality methods (Goddard et al., 2016; Goddard et al., 2019; Karimi-Rouzbahani et al., 2019), the connectivity method developed here allowed us to check whether the transferred signals contained *specific aspects of stimulus information*. Alternatively, it could be the case that the transferred signals might carry highly abstract but irrelevant information between the source and destination areas, which can be incorrectly interpreted as connectivity (Anzellotti and Coutanche, 2018; Basti et al., 2020). Briefly, feed-forward information flow is quantified as the degree to which the information from peri-occipital electrodes contributes to the information recorded at peri-frontal electrodes at a later time point, which reflects moving the frontal representation closer to that required for task goals. Feedback flow is defined as the opposite: the contribution to information at peri-frontal electrodes to that recorded later at peri-occipital electrodes (Figure 4A).

The results show that at the highest coherence level (55%), information flow is dominantly in the feed-forward direction. This is illustrated by the shaded area in Figure 4B where partialling out the peri-frontal from peri-occipital correlations only marginally reduces the total peri-occipital correlation (Figure 4B, black curves and shaded area), meaning that there is limited information transformation from peri-frontal to peri-occipital. In contrast, partialling out the peri-occipital from peri-frontal correlations leads to a significant reduction in peri-frontal correlation, reflecting a feed-forward exchange of information (Figure 4B, brown curves and shaded area). This trend is also seen for response-aligned analysis.

These differences are shown more clearly in Figure 4C where the peaks of feed-forward and feedback curves show that the feed-forward information is dominant earlier, followed by feedback information flow, as shown by the later peak of feedback dynamics. These results suggest that when the sensory evidence is high, feed-forward information flow may be sufficient for categorical representation and decision making while feedback only slightly enhances the representation. However, in lower coherence levels (i.e., low sensory evidence), the strength of information flow is either equivalent between feed-forward and feedback directions (30%, 45%) or dominantly feedback (22%, Figure 4D).

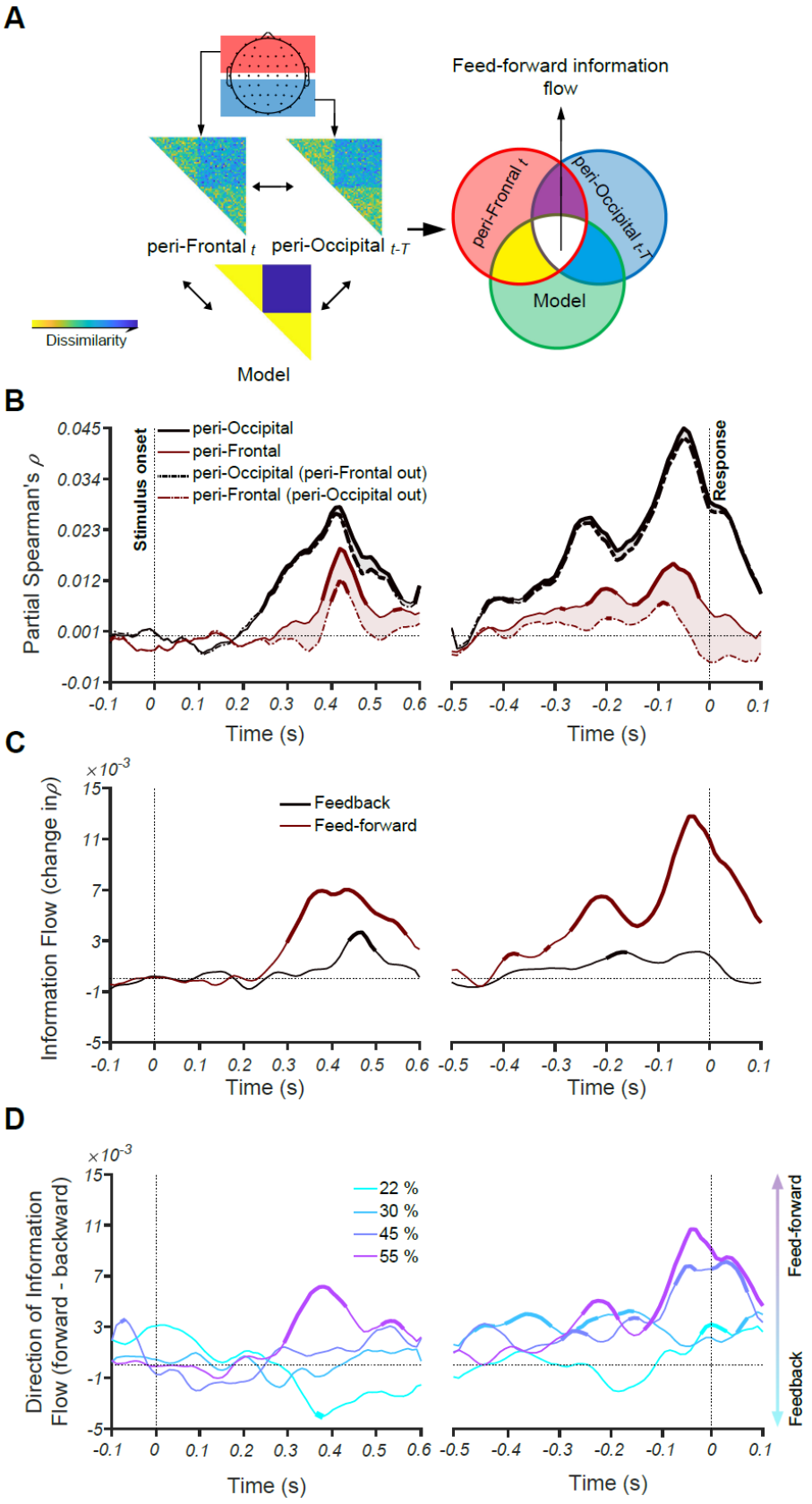

353

Figure 4. Feed-forward and feedback information flow revealed by RSA. (A) A schematic presentation of the method for calculating informational connectivity between the peri-frontal and peri-occipital electrodes, termed feed-forward and feedback information flow. Feed-forward information flow is calculated as the correlation between the *present* peri-frontal neural RDM and the predicted model RDM minus the same correlation when the *earlier* peri-occipital neural RDM is partialled out from it. **(B)** Time course of partial Spearman's correlations representing the partial correlations between the peri-occipital (black) and peri-frontal (brown) EEG electrodes and the model (see the inset in A) while including (solid) and excluding (dashed) the effect of the other area at phase coherence of 55%. The shaded area shows the decline in partial correlation of the current area with the model after excluding (partialling out) the RDM of the other area. Note that in both the dashed and solid lines, the low-level image statistics are partialled out of the correlations, so we call them partial correlations in both cases. **(C)** Feedforward (brown) and feedback (black) information flows obtained by calculating the value of the shaded areas in the corresponding curves in B. **(D)** Direction of information flow for different coherence levels, determined as the difference between feed-forward and feedback information flow showed in C. Thickened lines indicate time points at which the difference is significantly different from zero (sign permutation test and corrected significance level at $p < 0.05$), and black dotted lines indicate 0 correlation. The left panels show the results for stimulus-aligned analysis while the right panels represent the results for response-aligned analysis.

Here, we can see that the lower sensory evidence correlates with greater engagement of feedback mechanisms, suggesting that feedback is recruited to boost task-relevant information in sensory areas under circumstances where the input is weak. Therefore, the dynamics and relative contribution of feedback and feed-forward mechanisms in the brain appear to vary with the sensory evidence / perceptual difficulty of the task.

Importantly, we also were interested in knowing whether the degree of familiarity changes the direction of information flow between the peri-frontal and peri-occipital brain areas. For this analysis, we collapsed the data across all coherence levels as we were interested in the impact of face familiarity on information flow. Accordingly, we generated a wide range of RDM models, which allowed us to evaluate how much information about each subcategory of familiar faces (i.e., famous, personally familiar and self), levels of familiar faces, all familiar faces as a group, and unfamiliar faces were transferred between the two brain areas (Figure 5). As the results show, when the data were aligned to stimulus onset, self, familiar and familiarity level models showed the highest amount of feed-forward flow of information starting to accumulate after the stimulus onset, reaching sustained significance ~500 ms. However, less familiar categories did not reach significance. In the response-aligned analysis, again, the significant time points show the domination of feed-forward flow for the self, familiar and familiarity level models. Together,

these results suggest that while the information about the unfamiliar category could not evoke the domination of information in any directions, the representations of familiar, familiarity levels and self faces showed dominant feed-forward information flows from the peri-occipital to the peri-frontal brain areas. Note that, in this analysis, we also tried to minimize the effect of the participant's decision and motor response in the models by excluding the opposing category (i.e. unfamiliar category when evaluating the familiar models and *vice versa*), which potentially contributed to the information flows in the previous analysis.

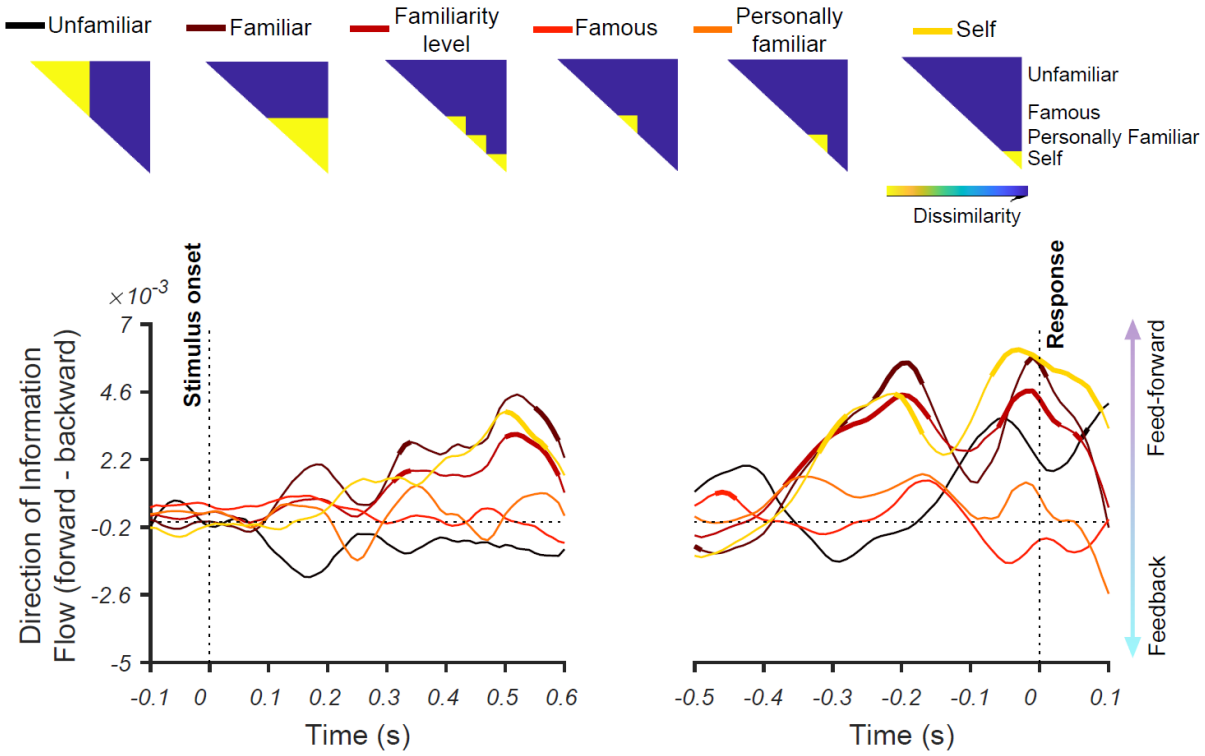

Figure 5. Directions of information flow for different familiarity levels using their corresponding RDM models. The models, as depicted on the top, are constructed to measure the extent and timing by which information about unfamiliar, familiar, familiarity levels and each familiar sub-category moves between the peri-occipital and peri-frontal brain areas. The yellow areas in the models refer to the target category (including unfamiliar, famous, self and personally familiar faces). Thickened lines indicate time points at which the difference is significantly different from zero (sign permutation test and corrected for multiple comparisons at significance level of $p < 0.05$), and black horizontal dotted lines indicate 0 correlation. The left panel shows the result for stimulus-aligned analysis while the right panels represent the result for response-aligned analysis.

Altogether, the results of the information connectivity analysis suggest that, in familiar face recognition, both top-down and bottom-up mechanisms play a role, with the amount of sensory evidence determining their relative contribution. It also suggests that the degree to which sensory information is processed feed-forward can be modulated by the familiarity level of the stimulus.

Discussion

This study investigated the neural mechanisms of familiar face recognition. We asked how perceptual difficulty and levels of familiarity affected the contribution of feed-forward and feedback processes in face processing. We first showed that manipulating the familiarity affected the informational content of neural responses about face category, in line with a large body of behavioral literature showing an advantage of familiar over unfamiliar face processing in the brain. Then, we developed a novel extension to informational connectivity analyses to track the exchange of familiarity information between peri-occipital and peri-frontal brain regions to see if frontal brain areas contribute to familiar face recognition. Our results showed that when the perceptual difficulty was low (high sensory evidence), the categorical face information was predominantly streamed through feed-forward mechanisms. On the other hand, when the perceptual difficulty was high (low sensory evidence), the dominant flow of face familiarity information reversed, indicating reliance on feedback mechanisms. Moreover, when teasing apart the effect of task and response from neural representations, only the familiar faces, but not the unfamiliar faces, showed the domination of feed-forward flow of information, with maximum flow for the most familiar category, the self faces.

Our results are consistent with the literature suggesting that visual perception comprises both feed-forward and feedback neural mechanisms transferring information between the peri-occipital visual areas and the peri-frontal higher-order cognitive areas (Bar et al., 2006; Summerfield et al., 2006; Goddard et al., 2016; Karimi-Rouzbahani et al., 2017b; Karimi-Rouzbahani et al., 2017c; Karimi-Rouzbahani et al., 2019). However,

previous experimental paradigms and analyses did not dissociate feedback and feed-forward information flow in familiar face recognition, and argued for a dominance of feed-forward processing (Dobs et al., 2019; di Oleggio Castello and Gobbini, 2015; Ellis et al., 1979; Young and Burton, 2018). The more nuanced view we present is important because stimulus familiarity, similar to other factors including levels of categorization (superordinate vs. basic level; Besson et al., 2017; Praß et al., 2013), task difficulty (Chen et al., 2008; Woolgar et al., 2015; Kay et al., 2017) and perceptual difficulty (Fan et al., 2020; Hupe et al., 1998; Gilbert and Li, 2013; Gilbert and Sigman, 2007; Lamme and Roelfsema, 2000; Woolgar et al., 2011), may affect the complex interplay of feed-forward and feedback mechanisms in the brain. Our results showed that the contribution of peri-frontal to peri-occipital feedback information was inversely proportional to the amount of sensory evidence about the stimulus. Specifically, we only observed feedback when the sensory evidence was lowest (high perceptual difficulty) in our face familairty categorization task. Although a large literature has provided evidence for the role of top-down feedback in visual perception, especially when sensory visual information is low, they generally evaluated the feedback mechanisms within the visual system (Ress et al., 2000; Lamme and Roelfsema, 2000; Super et al., 2001; Lamme et al., 2002; Pratte et al., 2013; Fenske et al., 2006; Lee and Mumford, 2003; Felleman et al., 1991; Delorme et al., 2004; Mohsenzadeh et al., 2018; Kietzmann et al., 2019) rather than across the fronto-occpital brain networks (Bar et al., 2006; Summerfield et al., 2006; Goddard et al., 2016; Karimi-Rouzbahani et al., 2018; Karimi-Rouzbahani et al., 2019). Our findings support theories suggesting that fronto-occipital information transfer may feedback (pre-existing) face templates, against which the input faces are compared for correct recognition (Bar et al., 2006; Summerfield et al., 2006). As an advantage to the previous results, which could not determine the content of the transferred signals (Bar et al., 2006; Summerfield et al., 2006; Goddard et al., 2016; Karimi-Rouzbahani et al., 2018; Karimi-Rouzbahani et al., 2019), using our novel connectivity analyses, we showed that the transferred signal contained information which contributed to the categorization of familiar and unfamiliar faces.

Despite methodological differences, our findings support previous human studies showing increased activity in lower visual areas when the cognitive and perceptual tasks

were difficult relative to easy, which the authors attributed to top-down contributions (Ress et al., 2000; Kay et al., 2017). However, due to the low temporal resolution of fMRI, these studies cannot show the temporal evolution of these top-down contributions or the validity of the hypothesized direction. Importantly, the observed increase in activity in lower visual areas does not necessarily correspond to the enhancement of neural representations in those areas - increased univariate signal does not show whether there is better / more information that will support performance. Electrophysiological studies in animals have also shown that cortical feedback projections robustly modulate responses of early visual areas when sensory evidence is low, or the stimulus is difficult to segregate from the background figure (Hupe et al., 1998). A recent study has also found cortical feedback modulated the activity of neurons in the dorsolateral geniculate nucleus (dLGN), which was less consistent when presenting simple vs. complex grating stimuli (Spacek et al., 2019). Therefore, varying perceptual difficulty seems to engage different networks and processing mechanisms, and we show here that this also pertains to faces: less difficult stimuli such as our high-coherence faces seem to be predominantly processed by the feed-forward mechanisms, while more difficult stimuli such as our low-coherence faces recruit both feed-forward and feedback mechanisms. However, the exact location of the feedback in all these studies, including ours, remains to be determined with the development of more accurate modalities for neural activity recording.

We observed that the direction of information flow is influenced by the familiarity of the stimulus. The models of familiar faces, familiarity levels and self faces, evoked a dominant flow of feed-forward information. The unfamiliar category, however, did not evoke information flow in any direction, as evaluated by our connectivity method. This is consistent with enhanced representations of familiar face categories in the feed-forward pathways (Dobs et al., 2019; di Oleggio Castello and Gobbini, 2015; Ellis et al., 1979; Young and Burton, 2018), which, in turn, requires less top-down contributions to facilitate the perception of relevant information (Bar et al., 2006; Gilbert and Sigman, 2007). Our results might initially seem inconsistent with Fan et al. 's (2020) study, which did not report significant differences between the temporal dynamics of familiar and unfamiliar face representations; however, they only used famous faces within the familiar face spectrum. In our sub-category analysis, we also did not observe differences between famous faces

and unfamiliar faces; our main findings were from highly familiar self faces. Overall, then, our results suggest that processing of familiar faces, especially the most familiar (self) faces, is dominated by feed-forward information flow.

Results also show that, in lower coherence levels, the information about the familiarity levels was generally stronger than the information about familiarity itself (as captured by familiar-unfamiliar model RDM; Supplementary Figure 1). This suggests a lower threshold for the appearance of familiarity level compared to familiar-unfamiliar representations, which are differentially developed through life-time experience and task instructions, resepectively. Specifically, development of neural representations reflecting familiarity levels could be a result of exposure to repetitive faces, which can lead to developing face-specific representations in the visual system (Dobs et al., 2019), while task instructions could temporarily enhance the processing of relevant information in the brain through top-down mechanisms (Hebart et al., 2018; Karimi-Rouzbahani et al., 2019). That is probably the reason for the dominance of feed-forward and feedback information flows in the processing of familiarity levels and familiar-unfamiliar information, respectively (Figure 5).

The RSA-based connectivity method used in this study further develops a recent shift towards multivariate brain connectivity methods (Anzellotti and Coutanche, 2018; Basti et al., 2020; Keitzmann et al., 2019; Goddard et al., 2016; Clarke et al., 2018; Karimi-Rouzbahani, 2018; Karimi-Rouzbahani et al., 2019; Karimi-Rouzbahani et al., 2020), and introduces several advantages over previous methods of connectivity analyses. Traditional connectivity methods examine inter-area interactions through indirect measures such as gamma-band synchronization (Gregoriou et al., 2009), shifting power (Bar et al., 2006) or causality in the activity patterns (Summerfield et al., 2006; Fan et al., 2020). Such connectivity methods consider simultaneous (or time-shifted) correlated activations of different brain areas as connectivity, but they are unable to examine how (if at all) relevant *information* is transferred across those areas. Goddard et al. (2016) developed an RSA-based connectivity method to solve these issues, which allowed us and others to track the millisecond transfer of stimulus information across peri-frontal and peri-occipital brain areas (Karimi-Rouzbahani, 2018; Karimi-Rouzbahani et al., 2019;

Goddard et al., 2019; Keitzmann et al., 2019). This method, however, has the limitation that, it cannot tell us *what* aspects of the representation are transferred and modulated. In other words, we need new methods to tell how (if at all) the transferred information is contributing to the representations in the destination area. Alternatively, we might find aspects of information which correlate the information in the source area and are observed in the destination of area with some delay, but do not show any contribution to the behavioural goals. To address this issue, Clarke et al., (2018), proposed an RSA-based informational connectivity method which incorporated RDM models, such as the ones that we used here, to track specific aspects of the transferred information. However, their method did not show the temporal dynamics of information flow across brain areas. Our novel connectivity analysis method allowed us, for the first time, to explicitly determine the *content*, the *direction* and the *temporal evolution* of the information transferred from the peri-frontal to peri-occipital areas and *vice versa*. The relevance of the transferred information is determined by the amount that the representations in the destination area are shifted towards our predefined predicted RDM models. In this way, we could determine the temporal dynamics of the contributory element of the transferred information. This informational connectivity method can be used to address questions about information exchange using a variety of multivariate brain imaging modalities. Note that, although the spatiotemporal flow of information observed in this study was obtained from familiar/unfamiliar face recognition data, a similar approach can be adopted to study the flow of information across a wide set of tasks, such as object recognition, target detection and image matching.

Our results specify the neural correlates for the behavioral advantage in recognizing more vs. less familiar faces in a “familiarity spectrum”. As in previous studies, our participants were better able to categorize highly familiar than famous or unfamiliar faces, especially in low-coherence conditions (Kramer et al., 2018; Young and Burton, 2018). This behavioral advantage could result from long-term exposure to variations of personally familiar faces under different lighting conditions and perspectives, which is usually not the case for famous faces. Our neural decoding results quantified a neural representational advantage for more familiar faces compared to less familiar ones (i.e. higher decoding for the former than the latter) to suggest that more familiar faces lead to

more distinguishable neural representations as well. Decoding accuracy was also proportional to the amount of sensory evidence: the higher the coherence levels, the higher the decoding accuracy. We observed that the decoding accuracy "ramped-up" and reached its maximum ~100 ms before participants expressed their decisions using a key press. These results are suggestive of sensory evidence accumulation and decision making processes during face processing in humans, consistent with previously reported data in monkey and recent single-trial ERP studies (Kelly et al., 2013; Hanks and Summerfield, 2017; Philiastides et al., 2006; Philiastides and Sajda, 2006; Shadlen and Newsome, 2001). The significant correlation between MVPA and our behavioral results, moreover, showed a direct relationship between neural representation and behavioral outcomes with regard to familiar face processing. This means that the behavioral advantages of self faces and the condition with the highest sensory evidence (highest coherence) could have been driven by the enhanced neural representations in those conditions.

The time courses of our EEG results showed their maximum effects after 400 ms post-stimulus onset, which makes our results incomparable to the previous studies, as these generally show face familiarity modulation during early ERP components such as N170, N250, and P300 (Dobs et al., 2019; Ambrus, 2019; Fan et al., 2020; Henson et al., 2008; Kaufmann et al., 2009; Schweinberger et al., 2002; Huang et al., 2017). Typically, these studies use event-related paradigms, which evoke initial brain activations peaking at around 200 ms, whereas our dynamic masking paradigm releases the information gradually along the time course of the trial. Moreover, the extended (>200ms) static stimulation used in previous studies has been suggested to bias towards domination of feed-forward processing (Goddard et al., 2016; Karimi-Rouzbahani, 2018), because of the co-processing of the incoming sensory information and the recurrence of earlier windows of the same input (Kietzmann et al., 2019; Mohsenzadeh et al., 2018), making it hard to measure feedback. However, our paradigm, while providing a delayed processing profile compared to previous studies, avoids this and also slows down the process of evidence accumulation so that it becomes more trackable in time.

In conclusion, our study demonstrates that the processing of face information involves both feed-forward and feedback flow of information in the brain, and which predominates depends on the strength of incoming perceptual evidence and the familiarity of the face stimulus. Our novel extension of multivairate connectivity analysis methods allowed us to disentangle feed-forward and feedback contributions to familiarity representation. This connectivity method can be applied to study a wide range of cognitive processes, wherever information is represented in the brain and transferred across areas. We also showed that the behavioral advantage for familiar face processing is robustly reflected in neural representations of familiar faces in the brain and can be quantified using multivariate pattern analyses. These new findings and methods emphasise the importance of, and open new avenues for, exploring the impact of different behavioral tasks on the dymanic exchange of information in the brain.

Materials and Methods

Participants

We recorded from 18 participants (15 male, aged between 20-26 years, all with normal or corrected-to-normal vision). Participants were students from the Faculty of Mathematics and Computer Science at the University of Tehran, Iran. All participants voluntarily participated in the experiments and gave their written consent prior to participation. All experimental protocols were approved by the ethical committee of the University of Tehran. All experiments were carried out in accordance with the guidelines of the Declaration of Helsinki.

Stimuli

We presented face images of four categories, including unfamiliar, famous, self and personally familiar faces. The unfamiliar faces (n=120) were unknown to participants. The famous faces (n=40) were pictures of celebrities, politicians, and other well-known people. These faces were selected from different, publicly available face databases[1]. In both categories, half of the images were female, and half were male. To ensure that all participants knew the famous face identities, participants completed a screening task prior to the study. In this screening, we presented them with the names of famous people in our data set and asked if they were familiar with the person.

The personally familiar faces were selected from participants' family, close relatives, and friends (n=40); self-images were photographs of participants (n=40). The images of self and personally familiar faces were selected to have varied backgrounds and appearances. On average, we collected n=45 for personally familiar and n=45 for self faces for every individual participant. All images were cropped to have 400×400 pixels and were converted to greyscale (Figure 1A). We ensured that spatial frequency, luminance, and contrast were equalized across all images. The magnitude spectrum of each image was adjusted to the average magnitude spectrum of all images in our database [2].

The phase spectrum was manipulated to generate noisy images characterized by their percentage phase coherence (Dakin et al., 2002). We used a total of four different phase coherence values (22%, 30%, 45%, and 55%), chosen based on behavioral pilot experiments, so overall behavioral performance spanned the psychophysical dynamic range. Specifically, the participants scored 52.1%, 64.7%, 85.2% and 98.7% in the mentioned coherence levels in the piloting. At each of the four phase coherence levels,

[1] http://mmlab.ie.cuhk.edu.hk/projects/CelebA.html
https://megapixels.cc/datasets/msceleb/
[2] https://github.com/Masoud-Ghodrati/face_familiarity

637 we generated multiple frames for every image: the number of frames generated
638 depended on the reaction time of the participants, as explained below.

639

640 EEG acquisition and Apparatus

641 We recorded EEG data from participants while they were performing the face
642 categorization task. EEG data were acquired in an electrostatically shielded room using
643 an ANT Neuro Amplifier (eego 64 EE-225) from 64 Ag/AgCl scalp electrodes and from
644 three periocular electrodes placed below the left eye and at the left and right outer canthi.
645 All channels were referenced to the left mastoid with input impedance <15k and chin
646 ground. Data were sampled at 1000 Hz and a software-based 0.1-200 Hz bandpass filter
647 was used to remove DC drifts, and high-frequency noise and 50 and 100 Hz (harmonic)
648 notch filters were applied to minimize line noise. These filters were applied non-causally
649 (using MATLAB filtfilt) to avoid phase-related distortions. We used Independent
650 Component Analysis (ICA) to remove artefactual components in the signal. The
651 components which were reflecting artefactual signals (eye movements, head
652 movements) were removed based on ADJUST's criteria (Mognon et al., 2011). Next, trials
653 with strong eye movement or other movement artifacts were removed using visual
654 inspection. On average, we kept 98.74%±1.5% artifact-free trials for any given condition.

655 We presented images on LCD monitor (BenQ XL2430, 24”, 144 Hz refresh rate,
656 resolution of 1920 ×1080 pixels) and the stimulus presentation was controlled using
657 custom-designed MATLAB codes and Psychtoolbox 3.0 (Brainard, 1997; Pelli, 1997). We
658 presented stimuli at a distance of 60 cm to the participant, and each image subtended 8°
659 × 8° of visual angle.

660

Procedure

Participants performed a familiar vs. unfamiliar face categorization task by categorizing dynamically updating sequences of either familiar or unfamiliar face images in two recording sessions (Figure 1A). Image sequences were presented in rapid serial visual presentation (RSVP) fashion at a frame rate of 60 Hz frames per second (i.e.,16.67 ms per frame without gaps). Each trial consisted of a single sequence of up to 1.2 seconds (until response) with a series of images from the same stimulus (i.e., selection from either familiar or unfamiliar face categories) at one of the four possible phase coherence levels. Importantly, within each phase coherence level, the overall amount of noise remained unchanged, whereas the spatial distribution of the noise varied across individual frames such that different parts of the underlying image was revealed sequentially. If stimuli are presented statically for more than ~200ms, this would result in a dominant feed-forward flow of information simply due to the incoming information (Goddard et al., 2016; Karimi-Rouzbahani, 2019; Lamme et al., 2000). On the other hand, if we present stimuli for very brief durations (e.g. < 50 ms), there may be insufficient time to evoke familiarity processing.

We instructed participants to fixate at the center of the monitor and respond as accurately and quickly as possible by pressing one of two keyboard keys (left and right arrow keys) to identify the image as familiar or unfamiliar using the right index and middle fingers, respectively. The mapping between familiar-unfamiliar categories and the two fingeres were swapped from the first session to the next (counterbalanced across participants) and the data were collapsed across the two sessions before analyses. As soon as a response was given, the RSVP sequence stopped, followed by an inter-trial interval of 1–1.2 s (random with uniform distribution). The maximum time for the RSVP sequence was 1.2 secs. If participants failed to respond within the 1.2 secs period, the trial was marked as a no-choice trial and was excluded from further analysis. We had a total of 240 trials (i.e., 30 trials per perceptual category, familiar and unfamiliar, each at four phase coherence levels) during the experiment. We presented six blocks of 36 trials each, and one block of 24 trials and participants had some resting time between the

blocks. Each image from the image set was presented to the participants once in each session.

Analysis

Decoding (MVPA) analysis

We decoded the information content of our conditions using Multivariate Pattern Analysis (MVPA) methods with Support Vector Machine (SVM) classifiers (Cortes et al., 1995). MVPA utilizes within-condition similarity of trials and their cross-condition dissimilarity to determine the information content of individual conditions. We trained an SVM classifier on the patterns of brain activity (from 64 EEG electrodes) from 90% of familiar (including personally familiar, famous, and self categories) and 90% of unfamiliar trials, and then tested the trained classifier on the left-out 10% of trials from each category. The classification accuracy from categorization of the testing data shows whether there is information about familiarity in the neural signal. We only used the trials in which the participant *correctly* categorized the stimulus as familiar or unfamiliar. We repeated this procedure iteratively 10 times until all trials from the two categories were used in the testing of the classifier once (no trial was included both in the training and testing sets in a single run), hence 10-fold cross-validation, and averaged the classification accuracy across the 10 validation runs. To obtain the decoding accuracy through time, we down-sampled the EEG signals to 100 Hz and repeated the same classification procedure for every 10 ms time point from -100 to 600 ms relative to the onset of the stimulus, and from -500 to 100 ms relative to the response. This allowed us to assess the evolution of face familiarity information relative to the stimulus onset and response separately.

To investigate the potential differences in the temporal evolution of the sub-categories contained in the familiar category (i.e., famous, personally familiar and self), we additionally calculated the decoding accuracy for each sub-category separately. Note that the same decoding results obtained from decoding of familiar vs. unfamiliar

717 categories were used here, only calculated separately for each sub-category of familiar
718 faces.

719 We used random bootstrapping testing to evaluate the significance of the decoding
720 values at every time point. This involved randomizing the labels of the familiar and
721 unfamiliar trials 10,000 times and obtaining 10,000 decoding values using the above
722 procedure. The p-values of the true decoding values were obtained as [1- p(randomly
723 generated decoding values which were surpassed by the corresponding true decoding
724 value)]. We then corrected the *p* values for multiple comparisons across time (using
725 MATLAB's mafdr function). After the correction, the true decoding values with $p < 0.05$
726 were considered significantly above chance (e.g., 50%).

727

728 Brain-behavior correlation

729 To investigate if the decoding results could explain the observed behavioral face
730 categorization results, we calculated the correlation between the decoding and the
731 behavioral results using Spearman's rank correlation. We calculated the correlation
732 between a 16-element vector containing the percentage correct behavioral responses for
733 the four coherence levels of the four familiarity levels (i.e. Familiar, Famous, Self and
734 Unfamiliar), and another vector with the same structure containing the decoding values
735 from the same conditions at every time point separately. Please note that here we
736 calculated the percentage correct for familiar and unfamiliar sub-categories in contrast to
737 what we did when plotting the behavioral accuracy for the whole experiment in Figure 1B.
738 To determine the significance of the correlations, the same bootstrapping procedure as
739 described above was repeated at every time point by generating 10,000 random
740 correlations after shuffling the elements of the behavioral vector. The true correlations
741 were compared with the randomly generated correlations and deemed significant if their
742 *p*-values (as computed above) were < 0.05 after correction for multiple comparisons.

743

Representational similarity analysis

Representational similarity analysis is used here for three purposes. First, to partial out the possible contributions of low-level image statistics to our decoding results, which is not directly possible in the decoding analysis (Supplementary Materials). Second, to investigate possible coding strategies that the brain might have adopted which could explain our decoding, specifically, whether the brain was coding familiar versus unfamiliar faces, the different levels of familiarity or a combination of the superordinate and subordinate categories. Third, to measure the contribution of information from other brain areas to the representations of each given area (see Information flow analysis).

We constructed neural representational dissimilarity matrices (RDMs) by calculating the (*Spearman's* rank) correlation between every possible representation obtained from every single presented image leading to a 240 by 240 RDM matrix. The matrices were constructed using signals from the electrodes over the whole brain as well as from peri-occipital and peri-frontal electrodes separately as explained later (Figures 4-6). We also constructed *image* RDMs for which we calculated the correlations between every possible pair of images which had generated the corresponding neural representations used in the neural RDMs. Finally, to evaluate how much the neural RDMs coded the familiar vs. unfamiliar faces and/or different familiarity levels, we constructed two models RDMs. In the *Familiar-Unfamiliar* model RDM, the elements which corresponded to the correlations of familiar with familiar, or unfamiliar with unfamiliar, representations (and not their cross-correlations) were valued as 1, and the elements which corresponded to the cross-correlations between familiar and unfamiliar faces were valued as 0. The *Familiarity level* model, on the other hand, was filled with 0s (instead of 1s) for the representations which corresponded to the cross-correlations between different sub-categories of familiar faces (e.g. personally familiar vs. famous) with everything else being the same as the *Familiar-Unfamiliar* model RDM. To correlate the RDMs, we selected and reshaped the upper triangular elements of the RDMs (excluding the diagonal elements) into vectors called 'RDV'. To evaluate the correlation between the neural RDVs and the model RDVs, we used *Spearman's* partial correlation in which we

calculated the correlation between the neural and the model RDV while partialling out the image RDV as in equation (1):

$$\partial correlation(t) = \rho RDV_{Neural}(t) RDV_{Model}.RDV_{Image}. \quad (1)$$

As indicated in the equation, the partial correlation was calculated for every time point of the neural data (10 ms time steps), relative to the stimulus onset and response separately using the time-invariant model and image RDVs. To evaluate the significance of the partial correlations, we used a similar bootstrapping procedure as was used in decoding. However, here we randomized the elements of the model RDV 10,000 times (while keeping the number of ones and zeros equal to the original RDV) and calculated 10,000 random partial correlations. Finally, we compared the true partial correlation at every time point with the randomly generated partial correlations for the same time point and deemed it significant if it exceeded 95% of the random correlations ($p < 0.05$) after correcting for multiple comparisons.

Informational connectivity analysis

We developed a novel model-based method of information flow analysis to investigate how earlier information content of other brain areas contributes to the present-time information content of a given area. While several recent approaches have suggested for information flow analysis in the brain (Goddard et al., 2016; Karimi-Rouzbahani, 2018; Karimi-Rouzbahani et al., 2019), following the recent needs for these approaches in answering neuroscience questions (Anzellotti and Coutanche, 2018), none of the previously developed methods could answer the question of whether the transferred information was improving the representation of the target area in line with the behavioral task demands. Our proposed model, however, explicitly incorporates the specific aspects of behavioral goals or stimuli in its formulation and allows us to measure

if the representations of target areas are shifted towards the behavioural/neural goals by the received information. An alternative would be that the incoming information from other areas are just epiphenomenal and are task-irrelevant. This new method can distinguish these alternatives.

Accordingly, we split the EEG electrodes in two groups, each with 16 electrodes: peri-frontal and peri-occipital (Figure 4A) to see how familiarity information is (if at all) transferred between these areas that can be broadly categorized as “cognitive” and “sensory” brain areas, respectively. We calculated the neural RDMs for each area separately and calculated the correlation between the neural RDV and the model RDV, partialling out the image RDM from the correlation (as explained in equation (1)). This resulted in a curve when calculating the partial correlation at every time point in 10 ms intervals (see the solid lines in Figure 4B). Note that the partial correlation curve for the peri-frontal area could have received contributions from the present and earlier representations of the same area (i.e., the latter being imposed by our sequential stimulus presentation). It could also have received contributions from earlier peri-occipital representations through information flow from peri-occipital to the peri-frontal area. To measure this potential contribution, we partialled out the earlier peri-occipital representations in calculation of the partial correlation between peri-frontal and model RDVs according to equation (2):

$$Peri-frontal\partial correlation(t) = \rho RDV_{Neural}(frontal,t)RDV_{Model}.\{RDV_{Image}, RDV_{Neural}(occipital,t-T)\}. \quad (2)$$

where $NeuralRDV(frontal,t)$ refers to the peri-frontal neural RDV at present and $NeuralRDV(occipital,t-T)$ refers to the peri-occipital neural RDV in an earlier time point. We then calculated the difference between the original partial correlation at the peri-frontal areas and the partial correlation calculated using equation (2) to determine the contribution of earlier peri-occipital representations we called this “contribution of

information feed-forward flow" (as indicated by the brown shades in Figure 4). To determine the contribution of the peri-frontal representations in moving the peri-occipital representations, we used equation (3):

$$Peri-occipital\partial correlation(t) = \rho RDV_{Neural}(occipital,t)RDV_{Model}.\{RDV_{Image},RDV_{Neural}(frontal,t-T)\}. \quad (3)$$

with the same notations as in equation (2). Accordingly, to determine the contribution of earlier peri-frontal representations in directing the peri-occipital representations towards the model RDV, namely 'contribution of information feedback flow', we calculated the difference between the original partial correlation at the peri-occipital areas (using equation (1)) and the partial correlation calculated using equation (3). In equations (1) and (2), the delay time (T) was considered 50 ms and the earlier representations were averaged in a 50 ms time window (including 5 RDVs obtained from 5 steps of 10ms intervals), according to the previously reported delay times between the peri-occipital and peri-frontal areas in visual processing (Foxe and Simpson, 2002, Karimi-Rouzbahani et al., 2019).

Finally, to characterize the information flow dynamics between the peri-occipital and peri-frontal areas, we calculated the difference between the feed-forward and feedback contribution of information flows. This allowed us to investigate the transaction of targeted information between the brain areas aligned to the stimulus onset and response. We repeated the same procedure using the Familiar-Unfamiliar as well as Familiarity level models to see if they differed. We determined the significance of the partial correlations using the above-explained random bootstrapping procedure. We determined the significance of the differences between partial correlations (the shaded areas in Figure 4 and the lines in panel C) and the differences in the feed-forward and feedback contribution of information using Wilcoxon's signed-rank test using $p < 0.05$ threshold for significance after correction for multiple comparisons (using Matlab mafdr).

Acknowledgements

We would like to thank Ali Yoonessi for supporting our electroencephalography data collection in his lab. We would also like to appreciate Chris I Baker and Mark Williams for revising the manuscript and providing their valuable feedback on this study.

References

Ambrus, Géza Gergely, Daniel Kaiser, Radoslaw Martin Cichy, and Gyula Kovács. 2019. “The Neural Dynamics of Familiar Face Recognition.” *Cerebral Cortex* 29 (11): 4775–4784.

Anzellotti, Stefano, and Marc N. Coutanche. 2018. “Beyond Functional Connectivity: Investigating Networks of Multivariate Representations.” *Trends in Cognitive Sciences* 22 (3): 258–269.

Bar, Moshe, Karim S. Kassam, Avniel Singh Ghuman, Jasmine Boshyan, Annette M. Schmid, Anders M. Dale, Matti S. Hämäläinen, Ksenija Marinkovic, Daniel L. Schacter, and Bruce R. Rosen. 2006. “Top-down Facilitation of Visual Recognition.” *Proceedings of the National Academy of Sciences* 103 (2): 449–454.

Basti, Alessio, Hamed Nili, Olaf Hauk, Laura Marzetti, and Richard Henson. 2020. “Multivariate Connectivity: A Conceptual and Mathematical Review.” *Neuroimage* 117179.

Besson, Gabriel, Gladys Barragan-Jason, Simon J. Thorpe, Michèle Fabre-Thorpe, Sébastien Puma, Mathieu Ceccaldi, and Emmanuel J. Barbeau. 2017. “From Face Processing to Face Recognition: Comparing Three Different Processing Levels.” *Cognition* 158: 33–43.

Brainard, David H. 1997. “The Psychophysics Toolbox.” *Spatial Vision* 10 (4): 433–436.

880 Chen, Yao, Susana Martinez-Conde, Stephen L. Macknik, Yulia Bereshpolova, Harvey
881 A. Swadlow, and Jose-Manuel Alonso. 2008. “Task Difficulty Modulates the Activity of
882 Specific Neuronal Populations in Primary Visual Cortex.” *Nature Neuroscience* 11 (8):
883 974.

884 Clarke, Alex, Barry J. Devereux, and Lorraine K. Tyler. 2018. “Oscillatory Dynamics of
885 Perceptual to Conceptual Transformations in the Ventral Visual Pathway.” *Journal of*
886 *Cognitive Neuroscience* 30 (11): 1590–1605.

887 Collins, Elliot, Amanda K. Robinson, and Marlene Behrmann. 2018. “Distinct Neural
888 Processes for the Perception of Familiar versus Unfamiliar Faces along the Visual
889 Hierarchy Revealed by EEG.” *NeuroImage* 181: 120–131.

890 Dakin, S. C., R. F. Hess, T. Ledgeway, and R. L. Achtman. 2002. “What Causes Non-
891 Monotonic Tuning of FMRI Response to Noisy Images?” *Current Biology* 12 (14):
892 R476–R477.

893 Delorme, Arnaud, Guillaume A. Rousselet, Marc J.-M. Macé, and Michele Fabre-
894 Thorpe. 2004. “Interaction of Top-down and Bottom-up Processing in the Fast Visual
895 Analysis of Natural Scenes.” *Cognitive Brain Research* 19 (2): 103–113.

896 Dobs, Katharina, Leyla Isik, Dimitrios Pantazis, and Nancy Kanwisher. 2019. “How Face
897 Perception Unfolds over Time.” *Nature Communications* 10 (1): 1–10.

898 Ellis, Hadyn D., John W. Shepherd, and Graham M. Davies. 1979. “Identification of
899 Familiar and Unfamiliar Faces from Internal and External Features: Some Implications
900 for Theories of Face Recognition.” *Perception* 8 (4): 431–439.

901 Fan, Xiaoxu, Fan Wang, Hanyu Shao, Peng Zhang, and Sheng He. 2020. “The Bottom-
902 up and Top-down Processing of Faces in the Human Occipitotemporal Cortex.” *ELife* 9:
903 e48764.

904 Felleman, Daniel J., and DC Essen Van. 1991. “Distributed Hierarchical Processing in
905 the Primate Cerebral Cortex.” *Cerebral Cortex (New York, NY: 1991)* 1 (1): 1–47.

Fenske, Mark J., Elissa Aminoff, Nurit Gronau, and Moshe Bar. 2006. “Top-down Facilitation of Visual Object Recognition: Object-Based and Context-Based Contributions.” *Progress in Brain Research* 155: 3–21.

Foxe, John J., and Gregory V. Simpson. 2002. “Flow of Activation from V1 to Frontal Cortex in Humans.” *Experimental Brain Research* 142 (1): 139–150.

Gilbert, Charles D., and Mariano Sigman. 2007. “Brain States: Top-down Influences in Sensory Processing.” *Neuron* 54 (5): 677–696.

Gilbert, Charles D., and Wu Li. 2013. “Top-down Influences on Visual Processing.” *Nature Reviews Neuroscience* 14 (5): 350–363.

Gobbini, M. Ida, Ellen Leibenluft, Neil Santiago, and James V. Haxby. 2004. “Social and Emotional Attachment in the Neural Representation of Faces.” *Neuroimage* 22 (4): 1628–1635.

Goddard, Erin, Thomas A. Carlson, and Alexandra Woolgar. 2019. “Spatial and Feature-Selective Attention Have Distinct Effects on Population-Level Tuning.” *BioRxiv*, 530352.

Goddard, Erin, Thomas A. Carlson, Nadene Dermody, and Alexandra Woolgar. 2016. “Representational Dynamics of Object Recognition: Feedforward and Feedback Information Flows.” *Neuroimage* 128: 385–397.

Gregoriou, Georgia G., Stephen J. Gotts, Huihui Zhou, and Robert Desimone. 2009. “High-Frequency, Long-Range Coupling between Prefrontal and Visual Cortex during Attention.” *Science* 324 (5931): 1207–1210.

Hanks, Timothy D., and Christopher Summerfield. 2017. “Perceptual Decision Making in Rodents, Monkeys, and Humans.” *Neuron* 93 (1): 15–31.

Hebart, Martin N., Brett B. Bankson, Assaf Harel, Chris I. Baker, and Radoslaw M. Cichy. 2018. “The representational dynamics of task and object processing in humans.” *Elife* 7: e32816.

Henson, Richard N., Elias Mouchlianitis, William J. Matthews, and Sid Kouider. 2008. "Electrophysiological Correlates of Masked Face Priming." *Neuroimage* 40 (2): 884–895.

Huang, Wanyi, Xia Wu, Liping Hu, Lei Wang, Yulong Ding, and Zhe Qu. 2017. "Revisiting the Earliest Electrophysiological Correlate of Familiar Face Recognition." *International Journal of Psychophysiology* 120: 42–53.

Hupé, J. M., A. C. James, B. R. Payne, S. G. Lomber, P. Girard, and J. Bullier. 1998. "Cortical Feedback Improves Discrimination between Figure and Background by V1, V2 and V3 Neurons." *Nature* 394 (6695): 784–787.

Johnson, Matthew R., Karen J. Mitchell, Carol L. Raye, Mark D'Esposito, and Marcia K. Johnson. 2007. "A Brief Thought Can Modulate Activity in Extrastriate Visual Areas: Top-down Effects of Refreshing Just-Seen Visual Stimuli." *Neuroimage* 37 (1): 290–299.

Karimi-Rouzbahani, Hamid, Alexandra Woolgar, and Anina N. Rich. 2020. "Neural signatures of vigilance decrements predict behavioural errors before they occur." *bioRxiv*.

Karimi-Rouzbahani, Hamid, Ehsan Vahab, Reza Ebrahimpour, and Mohammad Bagher Menhaj. 2019. "Spatiotemporal Analysis of Category and Target-Related Information Processing in the Brain during Object Detection." *Behavioural Brain Research* 362: 224–239.

Karimi-Rouzbahani, Hamid, Nasour Bagheri, and Reza Ebrahimpour. 2017a. "Average activity, but not variability, is the dominant factor in the representation of object categories in the brain." *Neuroscience* 346: 14–28.

Karimi-Rouzbahani, Hamid, Nasour Bagheri, and Reza Ebrahimpour. 2017b. "Hard-Wired Feed-Forward Visual Mechanisms of the Brain Compensate for Affine Variations in Object Recognition." *Neuroscience* 349: 48–63.

Karimi-Rouzbahani, Hamid, Nasour Bagheri, and Reza Ebrahimpour. 2017c. “Invariant Object Recognition Is a Personalized Selection of Invariant Features in Humans, Not Simply Explained by Hierarchical Feed-Forward Vision Models.” *Scientific Reports* 7 (1): 1–24.

Karimi-Rouzbahani, Hamid. 2018. “Three-Stage Processing of Category and Variation Information by Entangled Interactive Mechanisms of Peri-Occipital and Peri-Frontal Cortices.” *Scientific Reports* 8 (1): 1–22.

Kaufmann, Jürgen M., Stefan R. Schweinberger, and A. Mike Burton. 2009. “N250 ERP Correlates of the Acquisition of Face Representations across Different Images.” *Journal of Cognitive Neuroscience* 21 (4): 625–641.

Kay, Kendrick N., and Jason D. Yeatman. 2017. “Bottom-up and Top-down Computations in Word-and Face-Selective Cortex.” *Elife* 6: e22341.

Kelly, Simon P., and Redmond G. O’Connell. 2013. “Internal and External Influences on the Rate of Sensory Evidence Accumulation in the Human Brain.” *Journal of Neuroscience* 33 (50): 19434–19441.

Kietzmann, Tim C., Courtney J. Spoerer, Lynn Sörensen, Radoslaw M. Cichy, Olaf Hauk, and Nikolaus Kriegeskorte. 2019. “Recurrence Required to Capture the Dynamic Computations of the Human Ventral Visual Stream.” *ArXiv Preprint ArXiv:1903.05946*.

Kramer, Robin SS, Andrew W. Young, and A. Mike Burton. 2018. “Understanding Face Familiarity.” *Cognition* 172: 46–58.

Lamme, Victor AF, and Pieter R. Roelfsema. 2000. “The Distinct Modes of Vision Offered by Feedforward and Recurrent Processing.” *Trends in Neurosciences* 23 (11): 571–579.

Lamme, Victor AF, Karl Zipser, and Henk Spekreijse. 2002. “Masking Interrupts Figure-Ground Signals in V1.” *Journal of Cognitive Neuroscience* 14 (7): 1044–1053.

983 Landi, Sofia M., and Winrich A. Freiwald. 2017. “Two Areas for Familiar Face
984 Recognition in the Primate Brain.” *Science* 357 (6351): 591–595.

985 Lee, Tai Sing, and David Mumford. 2003. “Hierarchical Bayesian Inference in the Visual
986 Cortex.” *JOSA A* 20 (7): 1434–1448.

987 Leibenluft, Ellen, M. Ida Gobbini, Tara Harrison, and James V. Haxby. 2004. “Mothers’
988 Neural Activation in Response to Pictures of Their Children and Other Children.”
989 *Biological Psychiatry* 56 (4): 225–232.

990 Mechelli, Andrea, Cathy J. Price, Karl J. Friston, and Alumit Ishai. 2004. “Where
991 Bottom-up Meets Top-down: Neuronal Interactions during Perception and Imagery.”
992 *Cerebral Cortex* 14 (11): 1256–1265.

993 Mognon, Andrea, Jorge Jovicich, Lorenzo Bruzzone, and Marco Buiatti. 2011.
994 “ADJUST: An Automatic EEG Artifact Detector Based on the Joint Use of Spatial and
995 Temporal Features.” *Psychophysiology* 48 (2): 229–240.

996 Mohsenzadeh, Yalda, Sheng Qin, Radoslaw M. Cichy, and Dimitrios Pantazis. 2018.
997 “Ultra-Rapid Serial Visual Presentation Reveals Dynamics of Feedforward and
998 Feedback Processes in the Ventral Visual Pathway.” *Elife* 7: e36329.

999 Pelli, Denis G. 1997. “The VideoToolbox Software for Visual Psychophysics:
1000 Transforming Numbers into Movies.” *Spatial Vision* 10 (4): 437–442.

1001 Philiastides, Marios G., and Paul Sajda. 2006. “Temporal Characterization of the Neural
1002 Correlates of Perceptual Decision Making in the Human Brain.” *Cerebral Cortex* 16 (4):
1003 509–518.

1004 Philiastides, Marios G., Roger Ratcliff, and Paul Sajda. 2006. “Neural Representation of
1005 Task Difficulty and Decision Making during Perceptual Categorization: A Timing
1006 Diagram.” *Journal of Neuroscience* 26 (35): 8965–8975.

1007 Praß, Maren, Cathleen Grimsen, Martina König, and Manfred Fahle. 2013. “Ultra Rapid
1008 Object Categorization: Effects of Level, Animacy and Context.” *PLoS One* 8 (6).

1009 Pratte, Michael S., Sam Ling, Jascha D. Swisher, and Frank Tong. 2013. “How
1010 Attention Extracts Objects from Noise.” *Journal of Neurophysiology* 110 (6): 1346–1356.

1011 Ramon, Meike, and Maria Ida Gobbini. 2018. “Familiarity Matters: A Review on
1012 Prioritized Processing of Personally Familiar Faces.” *Visual Cognition* 26 (3): 179–195.

1013 Ramon, Meike, Luca Vizioli, Joan Liu-Shuang, and Bruno Rossion. 2015. “Neural
1014 Microgenesis of Personally Familiar Face Recognition.” *Proceedings of the National*
1015 *Academy of Sciences* 112 (35): E4835–E4844.

1016 Ress, David, Benjamin T. Backus, and David J. Heeger. 2000. “Activity in Primary
1017 Visual Cortex Predicts Performance in a Visual Detection Task.” *Nature Neuroscience* 3
1018 (9): 940–945.

1019 Schweinberger, Stefan R., Esther C. Pickering, Ines Jentzsch, A. Mike Burton, and
1020 Jürgen M. Kaufmann. 2002. “Event-Related Brain Potential Evidence for a Response of
1021 Inferior Temporal Cortex to Familiar Face Repetitions.” *Cognitive Brain Research* 14 (3):
1022 398–409.

1023 Shadlen, Michael N., and William T. Newsome. 2001. “Neural Basis of a Perceptual
1024 Decision in the Parietal Cortex (Area LIP) of the Rhesus Monkey.” *Journal of*
1025 *Neurophysiology* 86 (4): 1916–1936.

1026 Spacek, Martin A., Gregory Born, Davide Crombie, Steffen A. Katzner, and Laura
1027 Busse. 2019. “Robust Effects of Cortical Feedback on Thalamic Firing Mode during
1028 Naturalistic Stimulation.” *BioRxiv*, 776237.

1029 Sugiura, Motoaki, Carlos Makoto Miyauchi, Yuka Kotozaki, Yoritaka Akimoto, Takayuki
1030 Nozawa, Yukihito Yomogida, Sugiko Hanawa, Yuki Yamamoto, Atsushi Sakuma, and
1031 Seishu Nakagawa. 2015. “Neural Mechanism for Mirrored Self-Face Recognition.”
1032 *Cerebral Cortex* 25 (9): 2806–2814.

1033 Summerfield, Jennifer J., Jöran Lepsien, Darren R. Gitelman, M. Marsel Mesulam, and
1034 Anna C. Nobre. 2006. “Orienting Attention Based on Long-Term Memory Experience.”
1035 *Neuron* 49 (6): 905–916.

Supèr, Hans, Henk Spekreijse, and Victor AF Lamme. 2001. “Two Distinct Modes of Sensory Processing Observed in Monkey Primary Visual Cortex (V1).” *Nature Neuroscience* 4 (3): 304–310.

Taylor, Margot J., Marie Arsalidou, Sarah J. Bayless, Drew Morris, Jennifer W. Evans, and Emmanuel J. Barbeau. 2009. “Neural Correlates of Personally Familiar Faces: Parents, Partner and Own Faces.” *Human Brain Mapping* 30 (7): 2008–2020.

Visconti, M. di Oleggio Castello, and M. I. Gobbini. 2015. “Familiar Face Detection in 180 Ms.” *PloS One* 10 (8): e0136548–e0136548.

Woolgar, Alexandra, Adam Hampshire, Russell Thompson, and John Duncan. 2011. “Adaptive Coding of Task-Relevant Information in Human Frontoparietal Cortex.” *Journal of Neuroscience* 31 (41): 14592–14599.

Woolgar, Alexandra, Soheil Afshar, Mark A. Williams, and Anina N. Rich. 2015. “Flexible Coding of Task Rules in Frontoparietal Cortex: An Adaptive System for Flexible Cognitive Control.” *Journal of Cognitive Neuroscience* 27 (10): 1895–1911.

Young, Andrew W., and A. Mike Burton. 2018. “Are We Face Experts?” *Trends in Cognitive Sciences* 22 (2): 100–110.

Supplementary Materials

Low-level image statistics do not explain the separation of familiar from unfamiliar faces

Although, we did equalize the frequency content, pixel intensities and contrast of the images of our dataset (see *methods*), but we checked whether there are other low-level differences by creating a model representational dissimilarity matrix (RDM) for each of the categories under different phrase coherences. Briefly, *neural* RDMs are constructed by calculating the correlations (or dissimilarities) of the *brain* response to different face stimuli to give an abstract representation of information encoding in the brain. We also construct a *low-level feature* RDM, for which we calculate the correlations between images corresponding to each brain response. *Model* RDMs *predicted* representations in the brain (see *Methods*). The model RDMs were created for discriminating (1) familiar from unfamiliar (Supplementary Figure 1A) and also (2) the familiarity levels from one another (Supplementary Figure 1B). We then computed partial Spearman's correlations between one of the models and neural RDMs for every time point and participant, while partialling out (Supplementary Figure 1)/not partialling out (Supplementary Figure 2) low-level feature model RDM .

This analysis revealed the emergence of familiarity representation (familiar vs. unfamiliar faces) at around 270 ms post-stimulus for the highest coherence level (55%, Supplementary Figure 1A). The onset of significant representation is slightly later for lower coherence levels (e.g., 45%, Supplementary Figure 1A), which may suggest the need for additional processing time required to evaluate the sensory evidence. Interestingly, while the dynamics of familiarity level representations also showed gradual accumulation of information (Supplementary Figure 1B), especially for the 45% and 55% coherence, the correlation values are generally higher for the model of familiarity level compared to familiar-unfamiliar (c.f. Supplementary Figure 1A). This suggests that there might be well-established neural mechanisms in the brain that discriminate levels of

familiarity so strongly that is not suppressed/dominated by the task (i.e. here familiar-unfamiliar) or the response of the participants. This could also be supported by the observation that, as opposed to the familiar-unfamiliar representations, for which the 55% coherence provided the most information (at least in the stimulus-aligned analysis), the familiarity level representations provided their highest information in lower coherence levels such as 45% (in both stimulus- and response-aligned analyses) and 30% or even 22% in the response-aligned analysis. Note that participants' task and response could have also potentially contributed to the analysis of face familiarity model as those factors matched the familiar-unfamiliar model used in Supplementary Figure 1A.

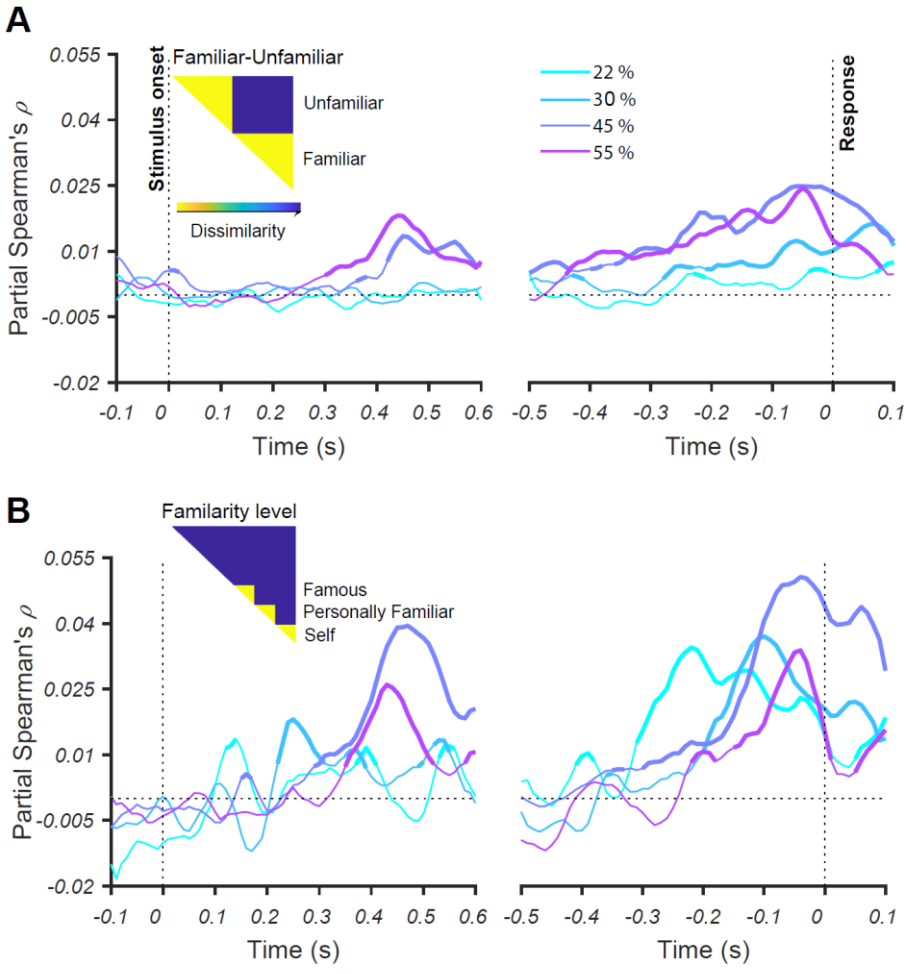

Supplementary Figure 1. Representations of face familiarity and categories revealed by RSA. Time course of Spearman's correlations between neural RDMs and model RDM (shown as insets) for (A) face familiarity; and (B) face familiarity levels, famous, self and personally familiar faces, after partialling out contributions from low-level features (see Methods). Each colored trace shows the correlations over time for one phase coherence level. Thickened lines indicate time points where the correlation is significant (sign permutation test, FDR-corrected significance level at $p < 0.05$), and black horizontal dotted lines indicate 0

correlation. The left panels show the results for stimulus-aligned analysis while the right panels represent the results for response-aligned analysis.

Apart from a small difference in absolute decoding rates, the dynamics of neural representations were similar when not partialling out the low-level feature model RDM (Supplementary Figure 2), presenting the ramping up of information, with earlier and most mounting trends for highest coherence levels (i.e. 45% and 55%). The similar patterns of neural information decoding between the correlation patterns with and without the low-level feature model suggest that low-level image statistics may only play a minor role in driving the observed decoding analyses. Nonetheless, we partialled out the low-level feature model in all the following RSA-based analyses to avoid their potential contribution to the results.

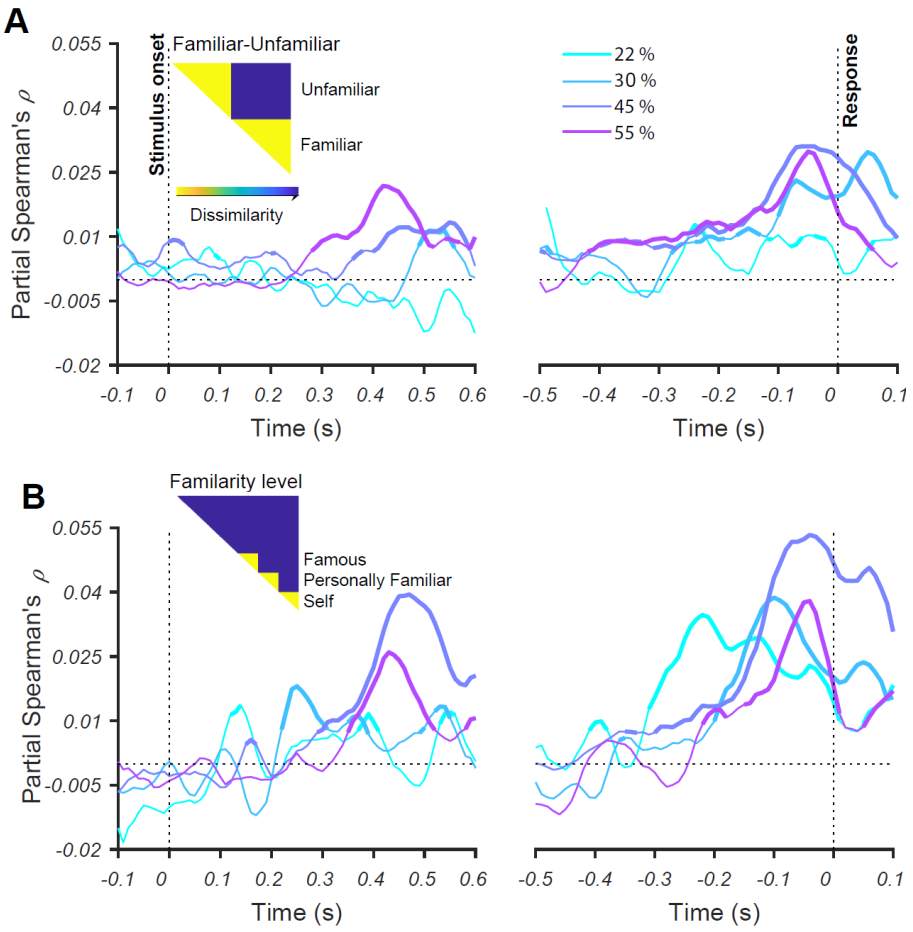

1115

1116 **Supplementary Figure 2. Representations of face familiarity and categories revealed by RSA.** Time
1117 course of Spearman's correlations between neural RDMs and model RDM (shown as insets) for (A) face
1118 familiarity; and (B) face familiarity levels, famous, self and personally familiar faces, before partialling out
1119 contributions from low-level features (see Methods). Each colored trace shows the correlations over time
1120 for one phase coherence level. Thickened lines indicate time points where the correlation is significant (sign
1121 permutation test, FDR-corrected significance level at $p < 0.05$), and black horizontal dotted lines indicate 0
1122 correlation. The left panels show the results for stimulus-aligned analysis while the right panels represent
1123 the results for response-aligned analysis. Note that the correlation values are higher compared to the results
1124 after partialling out contributions from low-level features (see Supplementary Figure 1).